17th World Conference on Earthquake Engineering, 17WCEE
Sendai, Japan - September 13th to 18th 2020
Paper N° XXXX (Abstract ID)
Registration Code: S-XXXXXXXX

NUMERICAL ANALYSIS ON AFTERSHOCK-INDUCED LIQUEFACTION OF SANDY GROUND WITH WATER-LEVEL RAISED BY MAIN SHOCK

T. Yoshikawa[(1)], T. Noda[(2)]

[(1)] *Assistant Professor, Nagoya University, yoshikawa.takahiro@b.mbox.nagoya-u.ac.jp*
[(2)] *Professor, Nagoya University, noda@nagoya-u.jp*

Abstract

In the 2011 off the Pacific coast of Tohoku Earthquake, extensive liquefaction damages were observed over a wide range of reclaimed coastal land. It is reported that, in Chiba prefecture, the big aftershock occurred 29 minutes after the main shock and it caused expanding the liquefaction damage in the sandy ground. Residents of the area testified that the water which had been oozing out from the ground due to the main shock was intensified by the aftershock. In this study, focusing on this resident witness and using a soil-water-air coupled elastoplastic finite deformation analysis code, it was shown that groundwater level rise induced by main shock may expand liquefaction damage during aftershock. To this end, one-dimensional numerical simulations were conducted, in which balances of pore water and pore air were easily comprehended. The initial groundwater level was set at 2 m below the ground surface.

Firstly, through the contour figures of saturation degree in the simulations, it is shown that the groundwater level rose due to the earthquake during the main shock. With the rise of groundwater level, the mean skeleton stress decreased in the soil elements with high degrees of saturation. On the other hand, the mean skeleton stress remained relatively high in the soil elements with low degrees of saturation. The reason why the groundwater level rose due to the earthquake was because the water drained due to consolidation (plastic volume compression) of the saturated ground was supplied to the shallow unsaturated ground and the water level rose by the volume of unsaturated soil (soil particles + pore water + trapped air) that sunk in the supplied water. Secondarily, it is shown in the simulation during the aftershock that saturation degree became higher just before the aftershock than just before the main shock, and consequently, the mean skeleton stress decreased more significantly during the aftershock than the main shock. Thus, one of the possibilities that the liquefaction damages expanded at the aftershock may be due to the groundwater level rise in the sandy ground caused by the main shock. In addition, the mechanism of groundwater level rise was clarified through case studies where material properties and initial conditions were varied.

Finally, it should be noticed that the phenomenon of groundwater level rise during/after an earthquake cannot be described by the elastic analysis, because it occurs as a result of plastic volume compression of the soil. Furthermore, it is necessary to determine the settlement precisely through sequential computation. Therefore, it needs to be emphasized that the analytical results described in this study could not have been obtained without using the soil-water-air three phase coupled elastoplastic finite deformation analysis.

Keywords: soil-water-air coupled finite deformation analysis, elastoplastic constitutive model, liquefaction, aftershock

1. Introduction

Widespread liquefaction damage was observed in reclaimed coastal land along Tokyo Bay during the 2011 off the Pacific coast of Tohoku Earthquake. The damage was particularly severe in Urayasu City, Chiba Prefecture, though the peak ground acceleration observed, around only 150 gal. The severe damage was attributed to the long duration of the earthquake and the aftershock that occurred 29 minutes after the main shock. Residents of the area have testified that the water which had been oozing out from the ground due to the main shock was intensified by the aftershock [1]. Studies on liquefaction during aftershocks have been carried out exclusively from the standpoint of a soil-water two phase system. For example, Nakai et al. [2] showed that the extended liquefaction damage could be attributed to the fact that excess pore water pressure which had risen during the main shock did not dissipate before the aftershock. In another study, Morikawa et al. [3] pointed out the effect of stress-induced anisotropy development that occurred during the main shock.

This paper describes a study performed from the standpoint of a soil-water-air three phase coupled analysis to determine the mechanism of the extended liquefaction damage caused by aftershocks. By simulating the series of events from a main shock to an aftershock using the soil-water-air coupled finite deformation analysis code [4], it is demonstrated that shallow unsaturated sandy ground becomes saturated by the rise in groundwater level caused by the main shock and that the aftershock results in the liquefaction in this saturated area. In addition, in order to clarify the mechanism of groundwater level rise, case studies were conducted where material properties and initial conditions were varied.

2. Analytical conditions

The finite element mesh used for analysis is shown in Fig. 1. One-dimensional analysis using the single transverse element mesh was carried out in this study so that the flow balances of water and air could be easily determined, assuming periodic boundary conditions in the lateral direction and viscous boundary conditions [5] at the bottom face. Assuming a ground depth of 20 m, the initial groundwater level was set at 2 m below the ground surface. The initial pore water pressure at the groundwater level was made to coincide with the pore air pressure, and vertically from there, a hydrostatic pressure distribution was assumed. At locations deeper than the groundwater level, the initial pore air pressure was set to be equal to the pore water pressure since suction is zero. At locations shallower than the groundwater level, the initial pore air pressure was set to zero at the initial ground surface and was distributed in the vertical direction based on the self-weight of air. The initial degree of saturation at locations deeper than the groundwater level was calculated according to the hydraulic pressure with consideration to the compressibility of air and water, assuming that the maximum degree of saturation of soil-water characteristic curve was at the groundwater level. The initial degree of saturation at locations shallower than the groundwater level was calculated according to the values for suction using the soil-water characteristic curve. The hydraulic/air boundary conditions assumed at the ground surface were constant total head condition corresponding to the initial groundwater level and exhausted condition (i.e., always at atmospheric pressure), respectively. All other boundaries were assumed to be in undrained and unexhausted conditions.

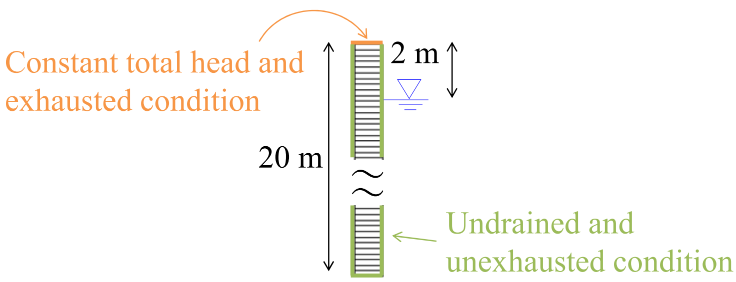

Fig. 1 – Finite element mesh

The soil material was assumed to be uniform across the entire region analyzed, and the material constants and initial values related to the elastoplastic constitutive equation, SYS Cam-clay model [6], were obtained from the mechanical experiments performed on soil samples from the alluvial sand ground in Urayasu City [7]. Since the filling soil and alluvial sand layers of the ground in Urayasu City contained a high content of fine fractions, the material constants related to the unsaturated seepage characteristics were determined by reference to the existing experimental results for clayey sand [8]. The material constants and initial values related to the SYS Cam-clay model and the unsaturated seepage characteristics are listed in Tables 1 and 2, respectively. Fig. 2 illustrates the soil water characteristic curve of this soil. The input seismic wave is illustrated in Fig. 3. The seismic wave recorded at the K-net Urayasu observation point (CHB008EW) during the 2011 off the Pacific coast of Tohoku Earthquake was modified by "SHAKE" using a model of the ground in the vicinity of the observation point to enable application to the bottom boundaries of the filling soil and alluvial sand layers. A half-wave of the modified seismic waveform was imposed at the bottom boundary in the horizontal direction. For simplicity, the same wave was used as the aftershock and was input 29 minutes after the main shock.

Table 1 – Material constants and initial values for the SYS Cam-clay model.

Elasto-plastic parameters		
Specific volume at q=0 and p'=98.1 kPa on NCL	N	2.0
Critical state constant	M	1.4
Compression index	$\tilde{\lambda}$	0.1
Swelling index	$\tilde{\kappa}$	0.0025
Poisson's ratio	ν	0.1
Evolution rule parameters		
Degradation index of overconsolidation	m	8.0
Degradation index of structure	a	8.0
Degradation index of structure	b, c	1.0
Degradation index of structure	c_s	1.0
Evolution index of rotational hardening	b_r	10.0
Limit of rotational hardening	m_b	0.44
Initial values		
Degree of structure	$1/R_0^*$	3.04
Overconsolidation ratio	$1/R_0$	Distributed
Void ratio	e_0	0.98
Stress ratio	η_0	0.545
Degree of anisotropy	ζ_0	0.0

Table 2 – Material constants and initial values for unsaturated seepage characteristic.

Soil water characteristic		
Maximum degree of saturation %	s^{w}_{max}	99.0
Minimum degree of saturation %	s^{w}_{min}	60.0
van Genuchten parameter kPa^{-1}	α	0.15
van Genuchten parameter (m' = 1-1/n')	n'	2.0
Saturated coefficient of water permeability m/s	k^{w}_{s}	5.0×10^{-4}
Dry coefficient of air permeability m/s	k^{a}_{d}	2.76×10^{-2}
Physical property		
Soil particle density g/cm^3	ρ^s	2.787
Bulk modulus of water kPa	K_w	2.19×10^{6}
Specific gas constant of air m^2/s^2/K	$\overline{R}$	287.04
Absolute temperature K	Θ	293.15

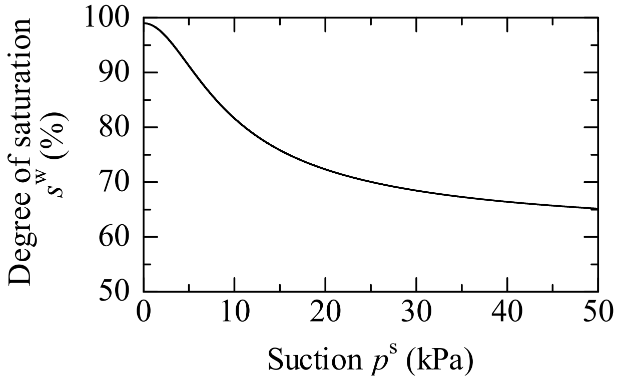

Fig. 2 – Soil water characteristic curve

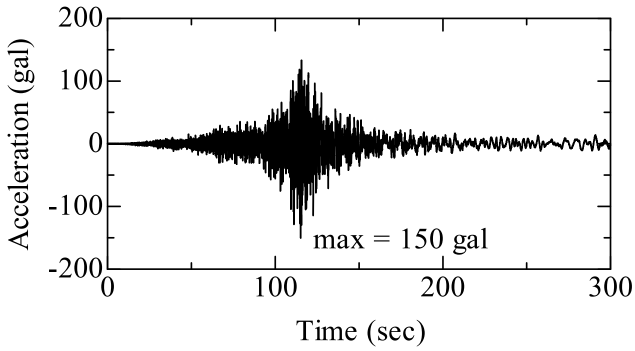

Fig. 3 – Input seismic wave

3. Analysis results

Fig. 4 depicts the distributions of saturation degree and mean skeleton stress just before and after the main shock. The contour figures were magnified to show the section of the ground up to about 2.5 m from its surface, including the part in which the initial groundwater level was located. It can be seen by comparing the distributions of saturation degree just before and after the main shock that the groundwater level rose during the main shock. With the rise of groundwater level, the mean skeleton stress can be seen to decrease in the soil elements with high degrees of saturation. On the other hand, the mean skeleton stress remained relatively high in the soil elements with low degrees of saturation near the ground surface. Fig. 5 shows the distribution of water content change just after the main shock. Due to drainage (plastic volume compression) in the part below the groundwater level, water absorption occurred near the ground surface, and the water content increased. That is, the water level rose. In this analysis, pore water movement occurred even during the earthquake because the duration of the earthquake was long and the coefficient of permeability was high.

Fig. 6 is a conceptual diagram showing the mechanism of groundwater level rise. First, consider one-dimensional consolidation of the saturated ground depicted in Fig. 6 (a) under drained upper boundary and undrained lower boundary conditions. Since the amount of ground settlement = the amount of water drained from the ground, the level of the supernatant water produced by drainage during consolidation is equal to the ground surface height before consolidation if we neglect the changes due to evaporation, rainfall, etc. In the current analysis, the part of the ground at or below the initial groundwater level was nearly saturated (degree of saturation = 99% or higher). This part underwent cyclic shearing during the earthquake and positive excess pore water pressure was generated due to negative dilatancy. As a result, consolidation settlement occurred through dissipation of excess water pressure. However, as shown in Fig. 6(b), when there is unsaturated soil above that part, the water drained by consolidation was supplied to the unsaturated soil. At this stage, because unsaturated soil is composed of soil particles, pore water, and pore air, the water level rose by the volume of soil (soil particles + pore water + trapped air) that sank in the portion corresponding to the supernatant water.

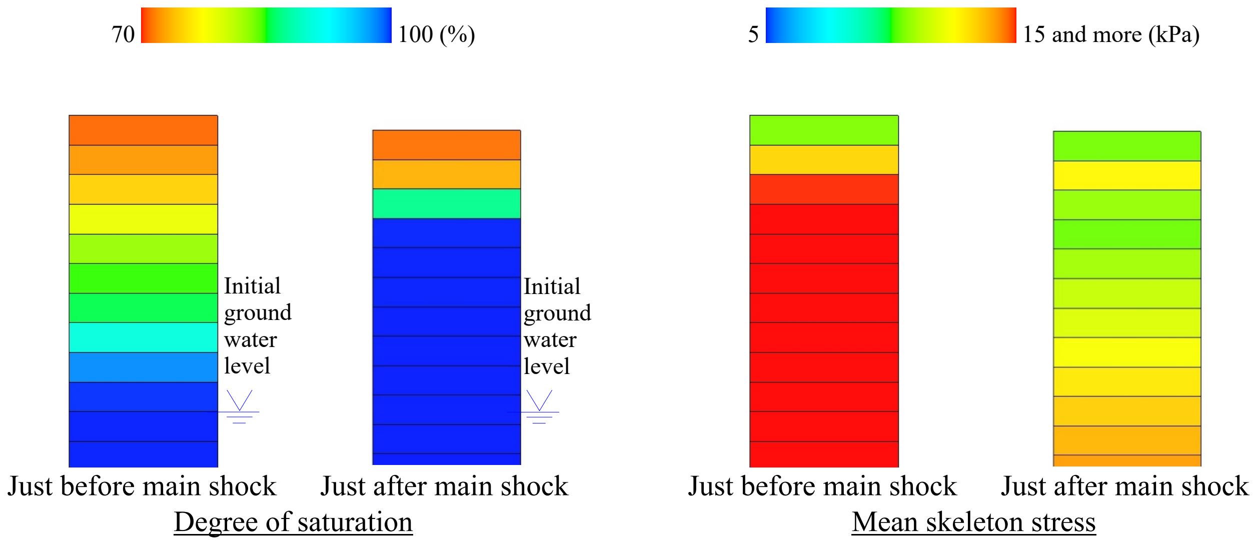

Fig. 4 – Comparison of saturation degree and mean skeleton stress between just before and after main shock

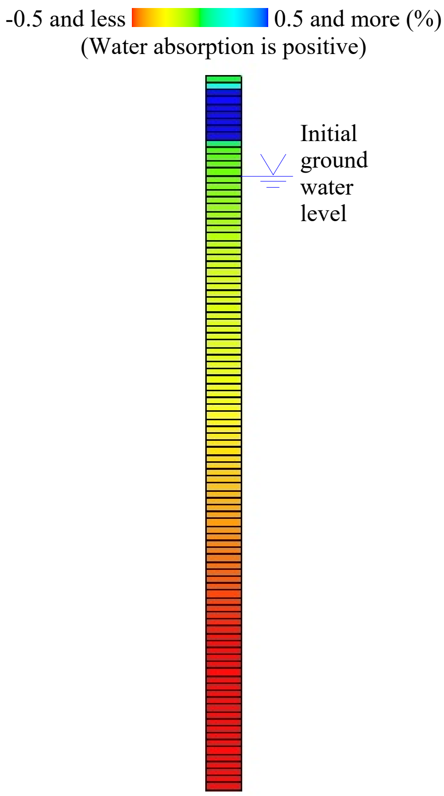

Fig. 5 – Water content change just after main shock from the initial state

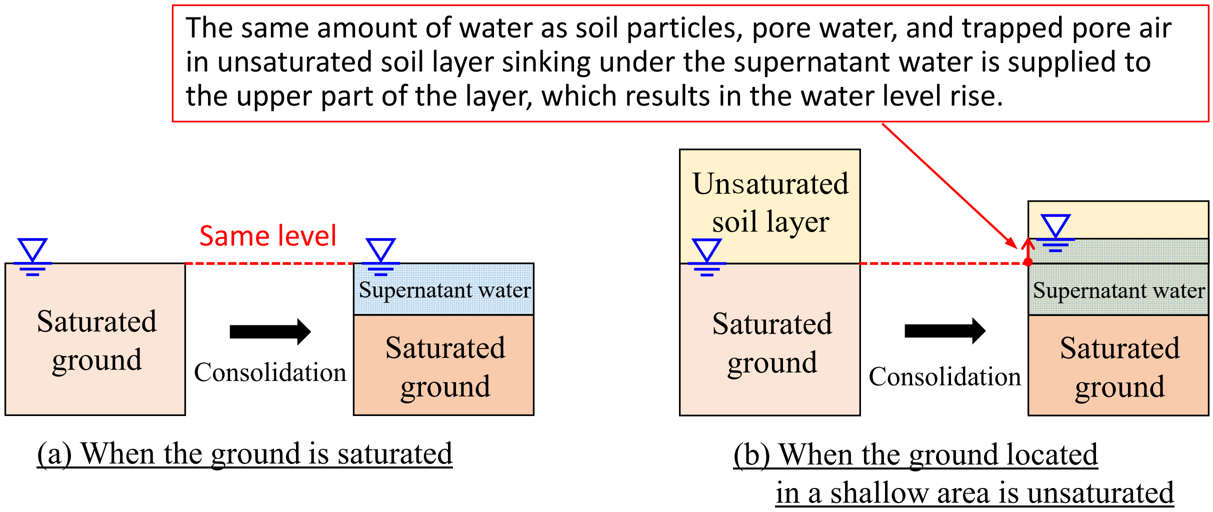

Fig. 6 – Schematic explanation of groundwater level rise mechanism

Fig. 7 depicts the distributions of saturation degree and mean skeleton stress just before and after the aftershock. Just before the aftershock, although the mean skeleton stress recovered due to the dissipation of excess pore water pressure, the degree of saturation near the ground surface rose further. Since the aftershock occurred in a state where the degree of saturation was high near the ground surface, the mean skeleton stress just after the aftershock decreased to a level lower than that after the main shock. In other words, one of the factors that causes the extended liquefaction during aftershocks may be the saturation of the unsaturated area near the ground surface due to a rise in groundwater level during and after the main shock.

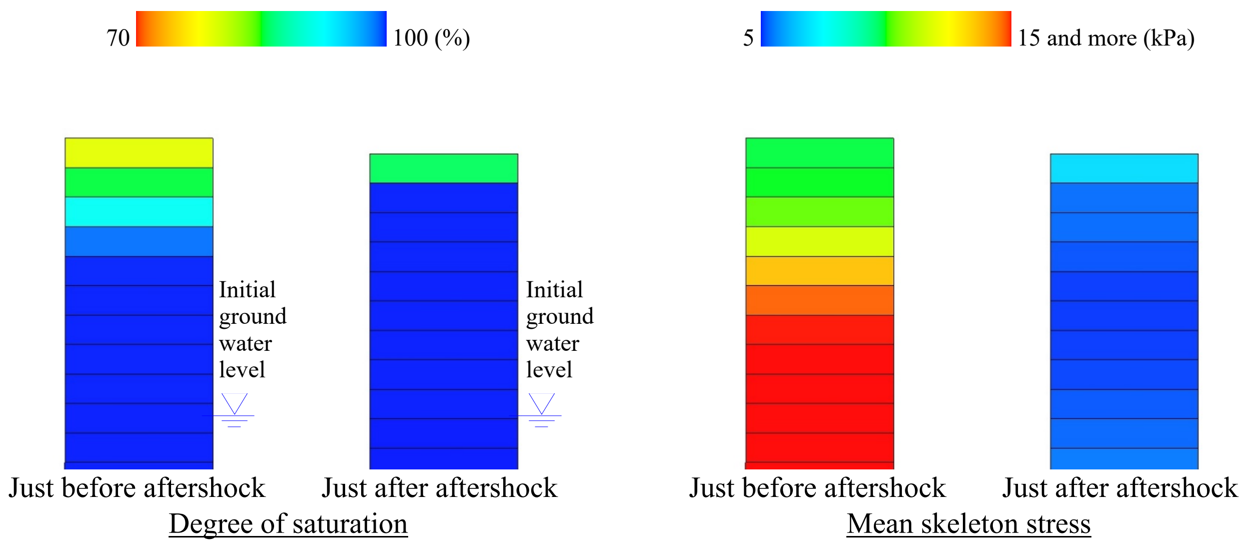

Fig. 7 – Comparison of saturation degree and mean skeleton stress between just before and after aftershock

4. Case study

Case studies were performed focusing on groundwater level rise. From the explanation in Fig. 6, the reason why groundwater level rises due to an earthquake is because the water drained due to consolidation of the saturated ground is supplied to the shallow unsaturated ground and the water level rises by the volume of unsaturated soil (soil particles + pore water + trapped air) sinking in the supplied water. Therefore, when a certain amount of drainage is generated due to consolidation of saturated ground and when unsaturated

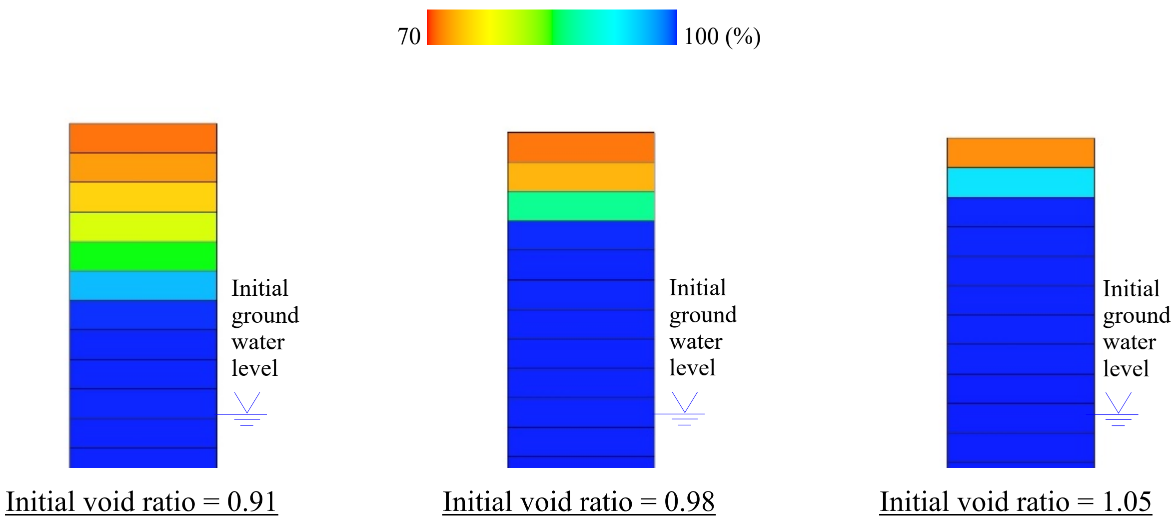

Fig. 8 – Comparison of saturation degree in grounds with different initial void ratio, just after the earthquake

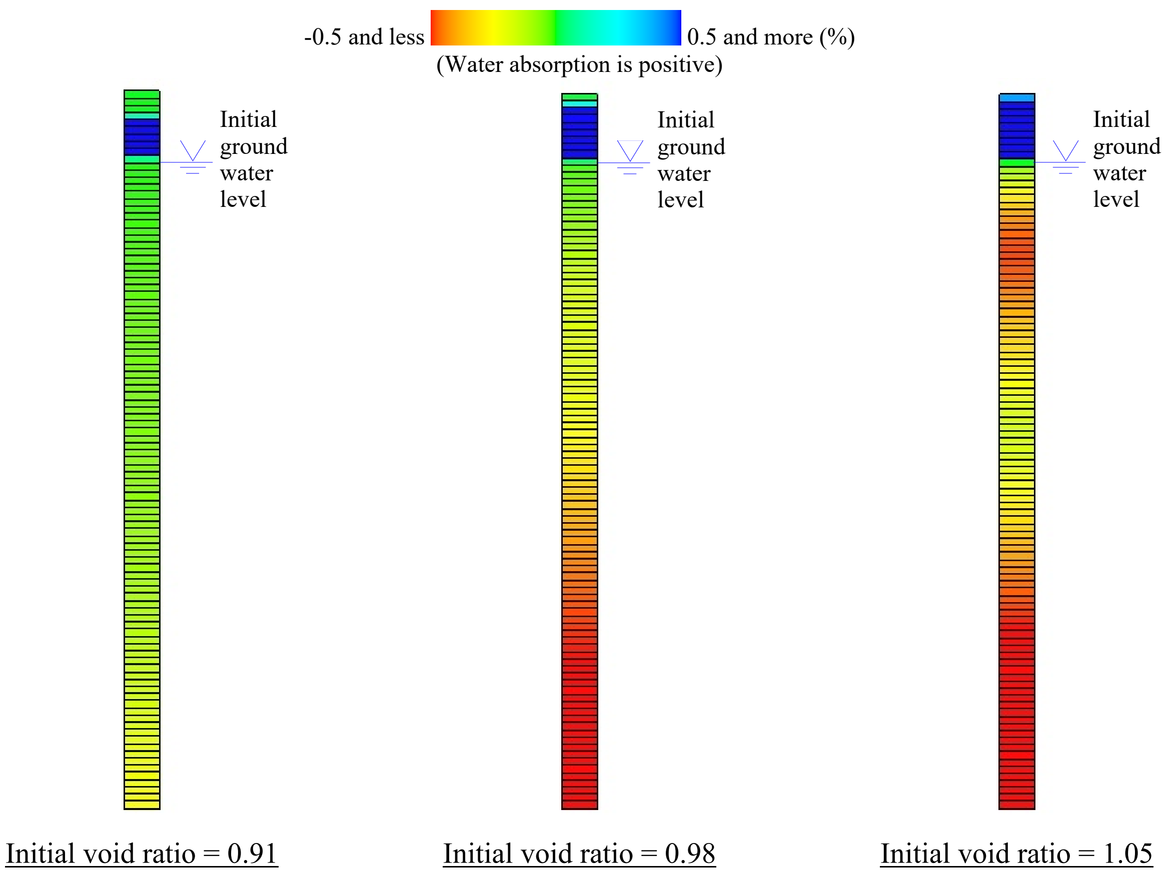

Fig. 9 – Comparison of water content change from the initial state in grounds with different initial void ratio, just after the earthquake

ground has the same initial saturation degrees, it may be expected that the smaller the void ratio, the higher the risen water level. Then, similar simulations were performed by changing the initial void ratio of the whole ground. Specifically, numerical simulations only during the main shock were conducted additionally for the ground with the initial void ratio of 0.91 and 1.05. Fig. 8 shows the comparison of saturation degree between just after the earthquake. Contrary to the above expectation, the water level rose higher when the inital void ratio was increased. Fig. 9 shows the distributions of water content change just after the earthquake. The larger the initial void ratio, the more the drainage from the saturated ground. When void ratio is large and soil is loose, the amount of consolidation drainage (plastic volume compression) increases; accordingly the water level rose higher when the inital void ratio was increased.

Next, numerical simulations were performed using elastic body and changing the initial void ratio only for the unsaturated part of the ground in order to make the effect of water level change easier to understand. That is, the unsaturated elastic bodies with the initial void ratio of 0.48, 0.98 and 1.48 above the initial groundwater level were used for the simulations, remaining the saturated part elasto-plastic body and its initial void ratio 0.98. Fig. 10 shows the contour figures of saturation degree. Unlike the case shown in Fig. 8, the smaller the void ratio of the unsaturated part, the higher the water level rose as expected. Because the plastic deformation (plastic volume compression) did not occur in the unsaturated elastic part, and consolidation drainage from the saturated ground is almost the same, the water level rises higher as void ratio in the unsaturated part becomes smaller. In addition, if the saturated part is also elastic, the water level does not change at all since the water level change is not caused by the plastic volume change.

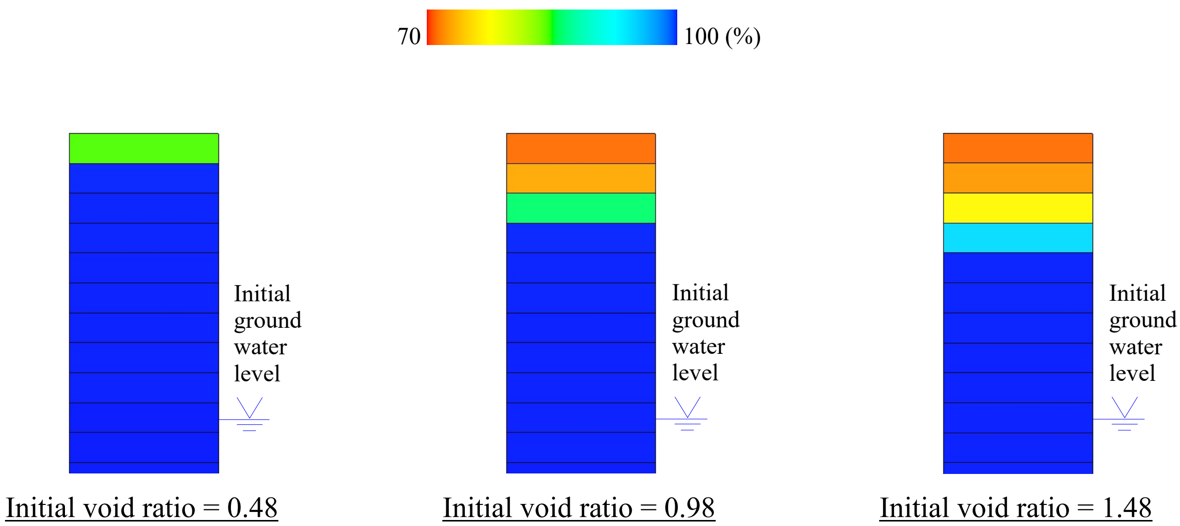

Fig. 10 – Comparison of saturation degree just after the earthquake among the grounds with unsaturated and elastic part above initial groundwater level, and with initial void ratio of 0.48, 0.98 and 1.48

5. Conclusion

The expansion mechanism of liquefaction during aftershocks was investigated by simulating the series of processes from a main shock to an aftershock using a soil-water-air coupled elastoplastic finite deformation analysis code. This study identified the following mechanisms. 1) Because of the external seismic forces, the saturated ground at and below the groundwater level is subjected to cyclic shear under the condition that drainage cannot take place immediately. As a result, excess pore water pressure is generated due to negative dilatancy. 2) If the duration of the earthquake is long, consolidation drainage accompanied with plastic volume compression occurs not only after but also during the earthquake. As a result, pore water is supplied from the saturated soil to the unsaturated soil above the groundwater level. 3) The groundwater level rises, and the saturated area expands between the main shock and aftershock. When the ground is subjected to the aftershock in such a state, the liquefied sand area becomes larger, resulting in extended liquefaction damage.

The phenomenon of groundwater level rise during an earthquake, which occurs as a result of plastic volume compression of the soil, cannot be described by an analysis that assumes soil to be an elastic body. Furthermore, it is necessary to determine the amount of settlement precisely through sequential computation. Therefore, it needs to be emphasized that the analytical results described in this paper could not have been obtained without using the soil-water-air three phase coupled elasto-plastic finite deformation analysis.

Acknowledgements

This work was supported by JSPS KAKENHI Grant Numbers JP25249064 and JP17H01289.

References

[1] Yasuda, S., Harada, K. and Ishikawa, K. (2012). Damage to structures in Chiba Prefecture during the 2011 Tohoku-Pacific Ocean Earthquake. Japanese Geotechnical Journal, 7(1), 103-115 (in Japanese).

[2] Nakai, K., Noda, T. and Asaoka, A. (2013). Main shock-aftershock interval effect on the liquefaction damage in Tohoku Region Pacific Coast Earthquake. Japan Geoscience Union Meeting 2013, SSS33-P24.

[3] Morikawa, Y., Bao, X., Zhang, F., Taira, A. and Sakaguchi, H. (2013). Why an aftershock with a maximum acceleration of 25 gal could make ground liquefied in the 2011 Great East Japan Earthquake. Proc. of 6th International Workshop on New Frontiers in Computational Geotechnics, 117-122.

[4] Noda, T. and Yoshikawa, T. (2015). Soil-water-air coupled finite deformation analysis based on a rate-type equation of motion incorporating the SYS Cam-clay model. Soils and Foundations, 55(1), 45-62.

[5] Lysmer, J. and Kuhlemeyer, R.L. (1969). Finite dynamic model for infinite media. ASCE, 95(EM4), 859-877.

[6] Asaoka, A., Noda, T., Yamada, E., Kaneda, K. and Nakano, M. (2002). An elasto-plastic description of two distinct volume change mechanisms of soils. Soils and Foundations, 42(5), 47-57.

[7] Nakai, K., Asaoka, A. and Sawada, Y. (2015). Liquefaction damage enhanced by interference between the body wave and surface wave induced from the inclined bedrock. Japanese Geotechnical Society Special Publication, 2(19), 723-728.

[8] Yamamoto, T., Nakai, T., Maruki, Y., Kodaka, T., Kishida, K. and Ohnishi, Y. (2009). Health assessment of the slopes along the roads introducing the long-term degradation concept. Japanese Geotechnical Journal, 4(1), 21-33 (in Japanese).